Carbohydrate Polymers 86 (2011) 239–244

Contents lists available at ScienceDirect

Carbohydrate Polymers

journal homepage: www.elsevier.com/locate/carbpol

Solubility of bacteria cellulose in zinc chloride aqueous solutions

Xinkun Lu, Xinyuan Shen*

State Key Laboratory for Modification of Chemical Fibers and Polymer Materials, College of Material Science and Engineering, Donghua University, Shanghai 201620, People's Republic of China

ARTICLE INFO

Article history:
Received 15 February 2011
Received in revised form 23 March 2011
Accepted 18 April 2011
Available online 27 April 2011

Keywords:
Bacterial cellulose
Zinc chloride aqueous solution
Dissolution
Wet-spin
RBC nascent fibers

ABSTRACT

Bacterial cellulose (BC) was dissolved in zinc chloride aqueous solution ($ZnCl_2{\cdot}3H_2O$) with a maximal concentration of 5.5 wt%, and regenerated bacteria cellulose (RBC) nascent fibers were spun with a wet-spinning process. The behavior of the BC/$ZnCl_2{\cdot}3H_2O$ solution was investigated, together with the structure and properties of the RBC nascent fibers. Results revealed that the BC/$ZnCl_2{\cdot}3H_2O$ solution showed typical shear thinning behavior. Though there was no chemical reaction occurred during the dissolution and spinning process, crystal forms of the RBC were transformed from cellulose I to cellulose II. Compared with the original BC fibers, the RBC fibers had lower degree of crystallinity and thermal stability, and showed round brilliants along the fiber axis with surface cracks and fibrillation, which caused lower tensile strength of 0.66–0.83cN/dtex, and extension at break of 1.95–3.66%.

1. Introduction

Recently, a new kind of cellulose source, bacterial cellulose (BC), also known as microbial cellulose, has emerged. BC, initially reported by Brown in 1886 (Brown, 1886), is a kind of unbranched polymer with the same β-1,4-linked glucopyranose residues as plant cellulose. But unlike the plant cellulose, BC consists of extremely fine fibrils and contains no biopolymers such as lignin, pectin, and hemicelluloses in the plant cellulose. Accordingly, BC has many excellent properties, such as unique nanostructure, high purity, high degree of polymerization, high crystallinity, biocompatibility, and biodegradability (Chen, Cho, & Jin, 2010a). Researches were made on its scientific applications on organic light emitting devices (Legnani et al., 2008; Nogi & Yano, 2008), food (Nguyena, Gidleyb, & Dykes, 2008), and medical material (Czaja, Young, Kawecki, & Brown, 2007; Maneerung, Tokura, & Rujiravanit, 2008; Zaborowska et al., 2010).

For more applications in different fields, researches should be made on solution of BC, as well as its regeneration, but further development is impeded for its poor solubility in common solvents. Up to now, much work has been focused on finding a good solvent for BC, and a few have been found which can be used to dissolve bacteria cellulose directly, e.g. lithium chloride/N,N-dimethylacetamide (LiCl/DMAc) (Chen, Kim, Kwon, Yun, & Jin, 2009; Shen, Ji, Wang, & Yang, 2010), NaOH/urea aqueous solution (Laskiewicz, 1998; Phisalaphong, Suwanmajo, & Sangtherapitikul, 2008), ionic liquids (Chen, Cho, & Jin, 2010b; Gericke, Schlufter, & Heinze, 2009), N-methylmorph-oline-N-oxide (NMMO) (Gao, Shen, & Lu, 2011). Furthermore, inorganic molten salts, which were cheap and environmentally friendly, were also used as efficient solvents for cellulose and its derivatization in a wide range of degrees of polymerization (Fischer, Leipner, Thümmler, Brendler, & Peters, 2003; Grinshpan et al., 1988; Leipner, Fischer, Brendler, & Voigt, 2000).

In this work, $ZnCl_2{\cdot}nH_2O$ was used as solvent of BC, and the RBC nascent fibers were spun with a wet-spinning process. The solubility of bacterial cellulose in $ZnCl_2{\cdot}nH_2O$ was investigated, together with the structure and properties of the prepared bacterial cellulose fibers.

2. Experimental

2.1. Raw materials

Bacterial cellulose in our experiments was supplied by Jiangsu Dengtai Bio-Technology (China) with the DP value of 4135 determined according to DIN 54270 applying copper (II)–ethylenediamine (Cuen) as solvent. Zinc chloride ($ZnCl_2$) was supplied by Sinopharm Chemical Reagent Co., Ltd.

The degree of polymerization (DP) of BC or RBC from the intrinsic viscosity was calculated according to the following equations (Heinze, Schwikal, & BarthelIonic, 2005):

$$\eta_{sp} = \frac{t - t_0}{t_0} = \eta_r - 1 \quad (1)$$

* Corresponding author. Tel.: +86 21 67792870; fax: +86 21 67792855.
E-mail address: shenxy@dhu.edu.cn (X. Shen).

0144-8617/$ – see front matter © 2011 Elsevier Ltd. All rights reserved.
doi:10.1016/j.carbpol.2011.04.042

$$[\eta] = \frac{\eta_{sp}}{C} \cdot \frac{1}{1 + k^m \eta_{sp}} \quad (2)$$

$$M_\eta = \left(\frac{[\eta]}{0.0116}\right)^{1/0.83} \quad (3)$$

$$\overline{DP} = \frac{M_\eta}{162} \quad (4)$$

η_r is the relative viscosity; η_{sp} is the specific viscosity; t_0 is the flow rate of the solution (s); t is the flow rate of the solvent (s); $[\eta]$ is the intrinsic viscosity ($ml\,g^{-1}$); C is the concentration of the solution ($g\,ml^{-1}$); k^m is the instrument constant $k^m = 0.29$.

2.2. Preparation of the solution

The preparation of the BC solution was carried out as follows. A certain amount of $ZnCl_2$ was dissolved in deionized water and put into a three-necked flask, and the flask was heated at 80 °C temperature.

Then, a certain amount of dried bacteria cellulose was added and stirred rapidly at different temperatures. The mixture gradually turned into a homogeneous solution. Every fifteen minutes, a few solution samples were taken out to observe the dissolved state of BC on XP51 optical polarized light microscope (Olympus Co., Japan). When the image had turned from colored to almost black, the transformation time was recorded. The influence was also examined of dissolution temperature and strength of the $ZnCl_2$, respectively.

2.3. Spinning

In this work, the wet spinning line used to produce the RBC nascent fibers was made by ourselves. Solution with the concentration of 5.0 wt% BC was spun at 50 °C and coagulated in different coagulation baths (absolute alcohol, acetone and 50% aqueous alcohol) at 20 °C to prepare RBC fiber I, II, III, with extrusion speed (V_1), pulling speed (V_2) and take-up speed (V_3) of 8.2 m/min, 3.5 m/min and 3.5 m/min, respectively. The collected fibers were washed in deionized water for about 24 h to remove residual solvent and dried under vacuum at 60 °C for 12 h.

2.4. Rheological measurements

The rheological measurements were made on RS150L Rotational rheometer (Thermo Haake, Karlsruhe, Germany), and a cone plate was used. The rheological properties of the BC/$ZnCl_2{\cdot}3H_2O$ solution were determined at 40 °C, 50 °C, 60 °C, 70 °C, 80 °C, respectively.

2.5. Fourier transform infrared spectroscopy (FT-IR) analysis

KBr slices of samples were prepared by mixing (1 mg) BC or regenerated BC fibers with 100 mg KBr (spectroscopic grade). The background spectrum was subtracted from the sample spectra. IR-spectra were recorded using a Fourier transform infrared spectrometer (FT-IR, Nicolet 8700, USA) in a spectral range of 400–4000 cm^{-1} at a resolution of 4 cm^{-1}. The scan speed was 0.2 cm/s and 32 scans were taken per sample.

2.6. Wide angle X-ray diffraction (XRD) analysis

The crystalline structure of the samples was examined using a wide angle X-ray diffractometer (D/max-2550 PC, Japan). The samples were scanned from $2\theta = 5$–60°, and the operating voltage and current were 40 kV and 200 mA, respectively. The radiation was Ni-filtered Cu-Ka radiation of wavelength 1.54056 Å.

2.7. Thermo gravimetric–differential thermal analysis

The TG instrument (TG 309F1, USA) was used in this study to test the changes of material mass loss and heat release with temperature. Test conditions were as follows: using an open aluminum sample cell in a nitrogen flow of 20 ml min^{-1} from 30 °C to 900 °C, using 2–3 mg as a standard for all samples, and 10 °C/min as the rate of increasing temperature. TG–DTA data were collected every second.

2.8. Mechanical properties

The single filament fineness was measured using a XQ-1 single filament fineness tester (Made in China), and mechanical properties of single fibers were measured using a XQ-1 single filament tenacity tester (Made in China), with a 20 mm gauge length at a crossbar rate of 20 mm/min. The tenacity and extension at break of the RBC fibers were calculated as the average of at least 25 measurements. All measurements were performed at room temperature and 65% relative humidity.

2.9. Microscopic analysis

Images of the regenerated fibers were taken by scanning electron microscopy (SEM) to observe the morphology and microstructure of the nascent fibers. The nascent fibers were frozen in liquid nitrogen, fractured immediately, and vacuum dried. The fracture surface of the fibers was also investigated. For SEM analysis, the fabric materials were sputtered with gold and then examined with a JSM 5600LV scanning electron microscope (JEOL, Tokyo, Japan), operated at 10 kV.

3. Results and discussion

3.1. Dissolution investigations of BC in $ZnCl_2{\cdot}nH_2O$

In order to determine the degree of polymerization (DP) of RBCs at different dissolution temperatures, the RBC films were coagulated in acetone and the viscometric degree of polymerization (DP_η) determined by viscosimetry in copper II ethylene diamine. In Table 1, with the dissolution temperature increasing, the viscometric degree of polymerization (DP_η) of the RBC descended sharply and the dissolution time also decreased obviously. Thermal degradation of DP was inevitable during the dissolving process at any convenient dissolution temperature. Taking all factors into consideration, 80 °C was chosen as the swelling and dissolution temperature. We also found that the BC sample would be gradually dissolved if placed at room temperature for some time long enough after full swelling at higher temperature (80 °C), which would be a better way to prevent the degradation of RBC and improve the properties of the RBC fibers.

The effects of water amount on solubility of BC in zinc chloride aqueous solutions were investigated too. For these systems, it was easy to find that the water amount strongly influences the dissolved BC in zinc chloride aqueous solutions. Results showed that, the $ZnCl_2{\cdot}4H_2O$ was a weak swelling agent, and the $ZnCl_2{\cdot}2H_2O$ with water amount of 2 mol per mol of the molten salt was a stronger swelling agent, and in molten $ZnCl_2{\cdot}3H_2O$, BC was swelled infinitely and dissolved completely with a maximal concentration of 5.5 wt%.

Fig. 1 shows the FT-IR spectra of the original BC and the RBC fibers. In Fig. 1, we could find that FT-IR spectra of the RBC fibers were similar to the original BC, which indicated that there was no significant difference between the structure of the original BC and RBC fibers. No chemical reaction had occurred during the dis-

Table 1
Effects of dissolution temperature of BC in zinc chloride aqueous solutions.

Solvent	Concentration (wt%)	Swelling temperature (°C)	Swelling time (min)	Dissolution temperature (°C)	Dissolution time (min)	DP_η
$ZnCl_2{\cdot}3H_2O$	3	–	–	75	210	1585
$ZnCl_2{\cdot}3H_2O$	3	–	–	80	135	2060
$ZnCl_2{\cdot}3H_2O$	3	–	–	85	105	1872
$ZnCl_2{\cdot}3H_2O$	3	–	–	90	75	1295
$ZnCl_2{\cdot}3H_2O$	3	–	–	95	60	855
$ZnCl_2{\cdot}3H_2O$	3	80	60	50	360	1638
$ZnCl_2{\cdot}3H_2O$	3	80	60	40	450	2204
$ZnCl_2{\cdot}3H_2O$	3	80	60	30	600	3196

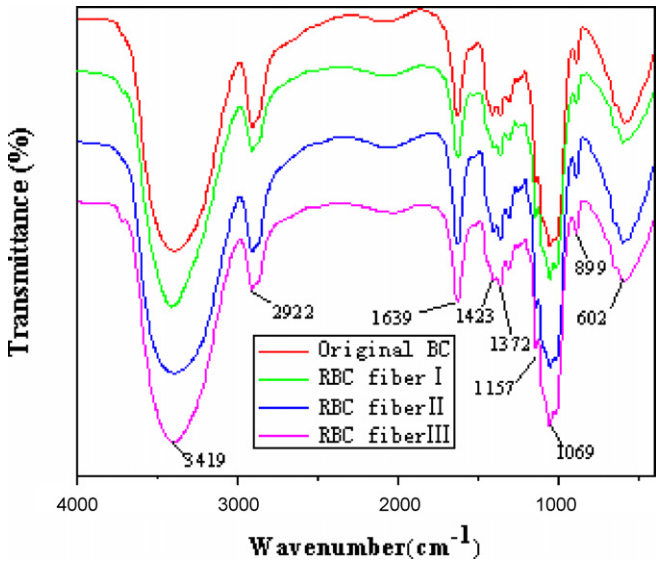

Fig. 1. FT-IR spectra of original BC and RBC fibers.

solution and coagulation processes of BC. There were only some physical changes during the whole process.

3.2. Rheological behavior of the BC/$ZnCl_2{\cdot}3H_2O$ solutions

Fig. 2a illustrated $\eta_a{\sim}\bar{\gamma}$ flow curves of BC/$ZnCl_2{\cdot}3H_2O$ solutions at different temperatures ($\bar{\gamma}$ was the shear rate and η_a was the apparent viscosity). The viscosity of the solution obviously decreased with an increase in $\dot{\gamma}$, which showed typical shear thinning behavior. Moreover, with the temperature increasing, the flow curve of the solution descended, and η_a showed a tendency to decline.

As we know, non-Newtonian index (n) was used to characterize the deviation degree of fluid from the Newtonian fluid. The n of the BC/$ZnCl_2{\cdot}3H_2O$ solutions were calculated by Eq. (5):

$$lg\,\sigma_\tau = lg\,K + n\,lg\,\dot{\gamma} \tag{5}$$

where σ_τ (Pa) was the shearing stress, $\dot{\gamma}$ (S^{-1}) was the shear rate, K was the viscosity coefficient and n was the non-Newtonian index. After making the $lg\,\sigma_\tau{\sim}lg\,\dot{\gamma}$ curves, it was easy to calculate the non-Newtonian index n, which was the slope of the curves. In Fig. 2b, all non-Newtonian indexes of BC/$ZnCl_2{\cdot}3H_2O$ solution (0.089–0.186) were much less than 1, suggesting that the BC solution belonged to false plastic fluid.

3.3. Crystal structure of the fibers

Fig. 3 shows the WAXD patterns of the original BC and RBC fibers. On the figure, original BC showed three strong Bragg peaks at about $2\theta = 14.46°$, 16.62° and 22.56° which were indexed as the (1 0 1), (1 0 $\bar{1}$) and (0 0 2) peaks of the typical cellulose I structure, respectively. We also found two strong Bragg peaks on XRD curve of RBC fiber I at about $2\theta = 12.26°$ and 20.70° which also could be indexed as the (1 0 1) and (1 0 $\bar{1}$) peaks of the cellulose II crystal structure respectively (Cai, Zhang, Guo, Shao, & Hu, 2010; Isogai, Usuda, Kato, Uryu, & Atalla, 1989; Zhang et al., 2009). The WAXD patterns of RBC fiber II and III were similar to fiber I.

In Table 2, it clearly demonstrated that the degree of crystallinity of the RBC fibers was about 40%, which was extremely lower than 73.17% of the original BC. It showed that the crystallite growth after regeneration was incomplete. There were similar crystal structures of the different RBC fibers prepared from different coagulation bath. Ethanol as the coagulation bath favored the crystallizing of RBC dur-

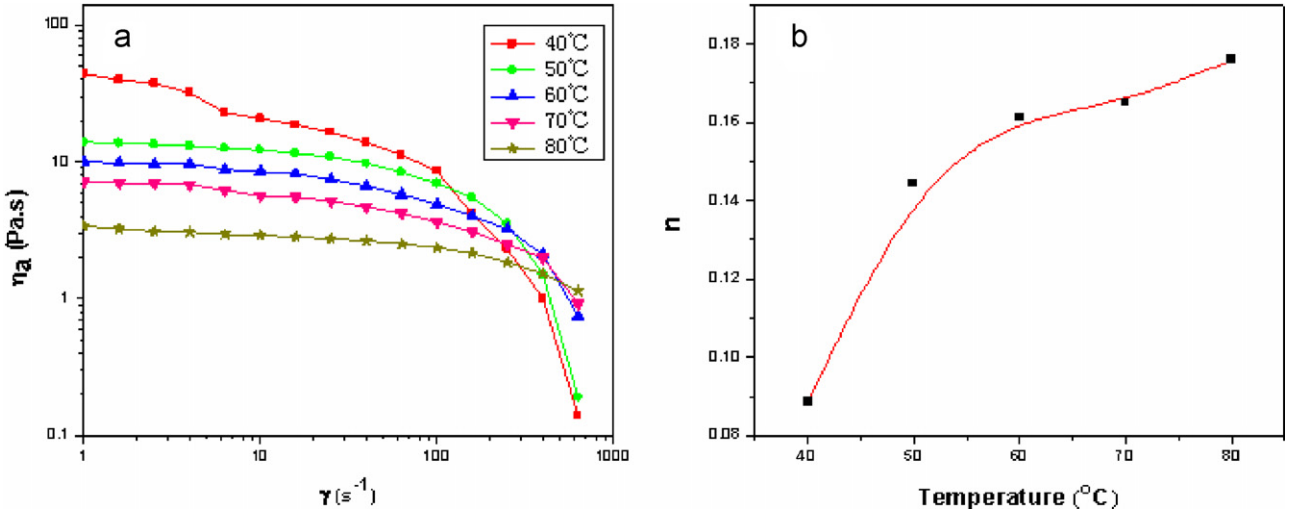

Fig. 2. Rheological behavior of 4% BC/$ZnCl_2{\cdot}3H_2O$ solutions at different temperatures: (a) flow curves and (b) non-Newtonian index n.

Table 2
The crystalline parameters of the original BC and RBC fibers.

Sample	Bragg peak I (°) (101)	Bragg peak II (°) $10\bar{1}$	Bragg peak III (°) (002)	Xc (%)	Crystal form
BC	14.460	16.620	22.560	73.17	Cellulose I
RBC fiber I	12.261	20.700	–	45.08	Cellulose II
RBC fiber II	12.685	20.702	–	40.52	Cellulose II
RBC fiber III	12.418	20.541	–	42.06	Cellulose II

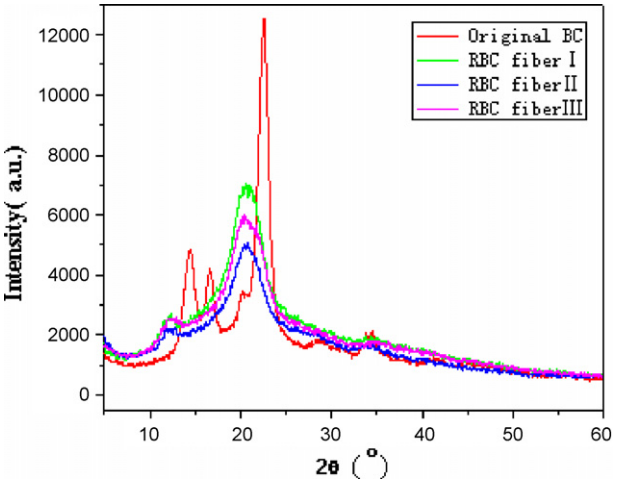

Fig. 3. WAXD patterns of the original BC and RBC fibers.

ing the whole spinning process. These results suggested that the crystal structures of the RBC fibers from different coagulation bath were transformed cellulose I into cellulose II after the dissolution and subsequent coagulation, which was similar to the transformation of the cellulose crystal structure in the lyocell process (Liu, Shen, Shao, Wu, & Hu, 2001).

3.4. Thermal behaviors of the fibers

Thermal behaviors of the original BC and RBC fibers were shown in Fig. 4. It is well known that the structural organization of polymers influences the shape of thermograms in thermal analysis of cellulose materials.

There were four-step degradations of BC. The mass losses, within 150 °C before the onset temperature, were related to water evaporation on the surface of BC. From 150 °C to 330 °C, the mass almost unchanged. Further weight loss (76.95%) from 330 °C to 371 °C was relatively fast, which was due to dehydration and decomposition of the molecules of BC. From 371 °C to 856 °C, the mass losses were slower and moderate. The mass decreased slightly again from 856 °C to 900 °C, with about 2% loss. However, the TG curves of the RBC fibers illustrated that the dehydration and decomposition of the molecules began at about 305 °C, and the residual masses of RBC fibers (3.97–8.77%) was more than BC (0.17%) at 900 °C, and the mass decreased only about 59% from 305 °C to 336 °C, which were less than BC. Furthermore, the onset temperatures of the RBC fibers were about 25 °C lower than the original BC. Higher onset temperatures were associated with higher thermal stability.

From Fig. 4b, the maximum degradations step at 352.3 °C for BC, 322.9 °C for RBC fiber I, 323.3 °C for RBC fiber II, and 324.5 °C for RBC fiber III were assigned to the bacteria cellulose degradation. All of above indicated that the thermal stability of the RBC fibers was slightly worse than the original BC.

3.5. Mechanical properties of the fibers

The mechanical properties of the RBC fibers from different coagulated bath were shown in Table 3. Results showed that absolute alcohol was the better coagulation bath for dissolution system, which had better tensile strength, initial modulus and elongation at break. However, it was also demonstrated that the RBC fibers possessed relatively poor tensile strength and elongation at break, indicating that they could not be used in industry directly. Thus, further work should be carried out to optimize the spinning parameters and improve the mechanical properties of the RBC fibers.

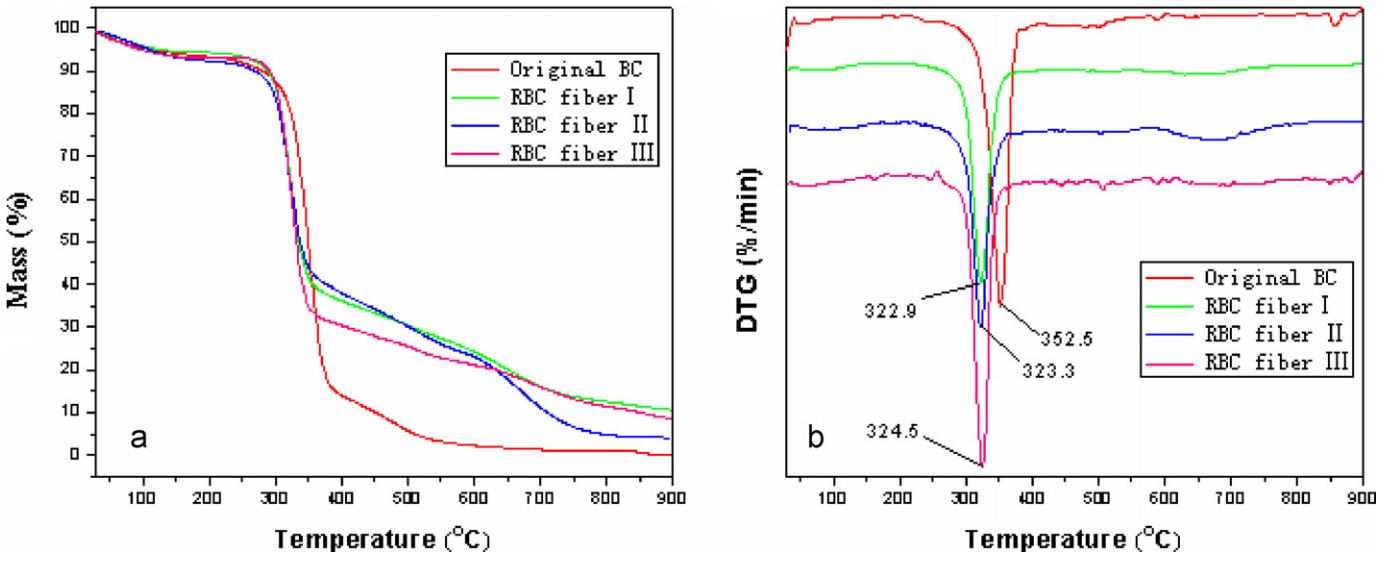

Fig. 4. TG (a) and DTG (b) curves of original BC and RBC fibers.

Table 3
Tenacity and extension at break RBC fibers from different coagulated bath.

Sample	Coagulation bath	Fiber fineness (dtex)	Tenacity (cn/dtex)	Elongation at break (%)	Modulus (cn/dtex)
RBC fiber I	CH_3CH_2OH	7.91	0.83	3.66	27.44
RBC fiber II	CH_3COCH_3	8.90	0.66	1.95	15.12
RBC fiber III	50%CH_3CH_2OH/H_2O	8.54	0.68	3.14	22.51

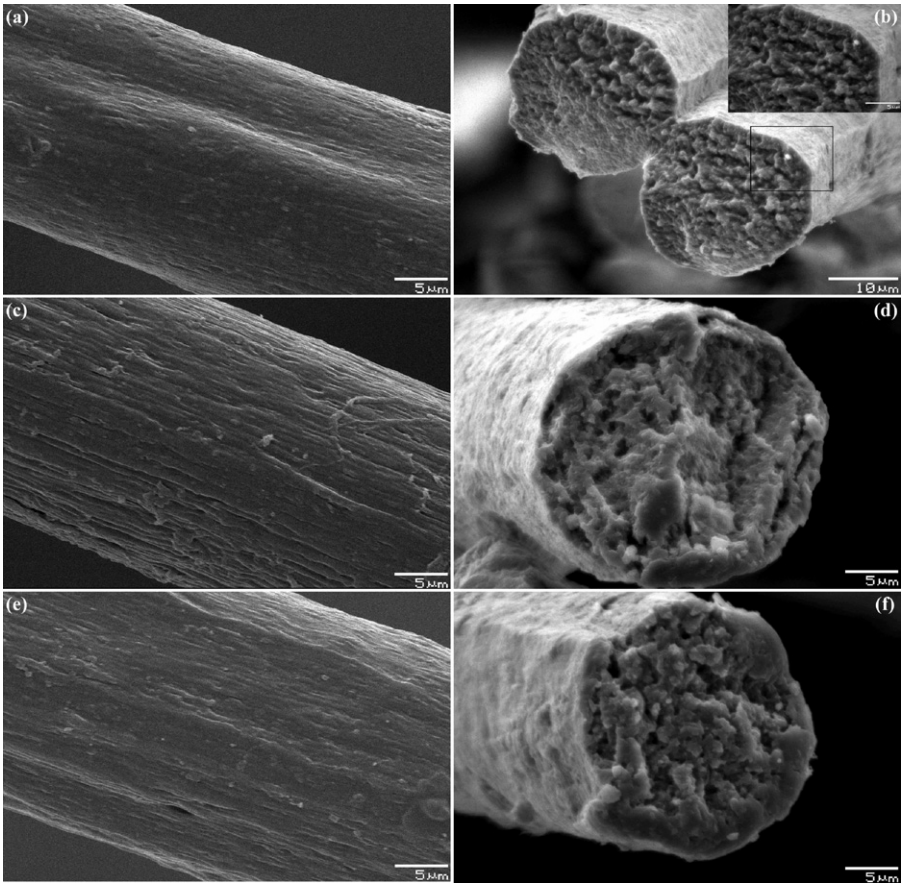

Fig. 5. SEM photographs of surface and cross section of the RBC fibers: picture (a, c, e) indicated the surface of RBC fiber I, II and III respectively (3000×), inset in picture (b) is a higher magnification image (5000×); picture (b, d, f) showed the cross-sections of RBC fiber I, II and III, respectively (3000×).

3.6. Morphology of the fibers

SEM analysis was used to characterize the structures on surface and cross section morphology of the RBC fibers. Representative SEM micrographs, taken with magnification of 3000 of the RBC fibers were shown in Fig. 5. Surfaces of the fibers on picture (a, c, e) were not smooth, with some slight longitudinal striations and flaws, which were conducive to later dyeing, but surface of RBC fiber I showed on picture (a) was smoother than RBC fiber II and III. From picture (b, d, f), it was easy to find that there were lots of voids on the cross-section of the fibers and a new compact cortex appeared in the fibers (showed in the enlarged image on picture (b) clearly). Large bundles or layers of macrofibrils were clearly observed on the cross section of the fibers. The whole fibers showed a loose and slight skin-core structure, which were the root cause of poor tensile strength and elongation at break of the RBC fibers. In addition, the cross section of the RBC fibers were as round as that of the lyocell fiber (Liu et al., 2001), and the whole fibers showed a circular shape along the fiber axis with the presence of surface cracks and fibrillation.

4. Conclusion

In this article, we discovered the molten salt hydrate, $ZnCl_2{\cdot}3H_2O$, was a kind of effective and efficient solvent for bacteria cellulose, which was cheap and environmentally friendly.

We dissolved BC in $ZnCl_2{\cdot}3H_2O$ at 80 °C and spun at 50 °C after comprehensive consideration. With typical shear thinning behavior, the BC/$ZnCl_2{\cdot}3H_2O$ solution was a kind of non-Newtonian fluid for the dissolution systems and belonged to false plastic fluid. Dissolution of bacteria cellulose in $ZnCl_2{\cdot}3H_2O$ and subsequent coagulation was accompanied with the transformation from cellulose I to II, and no significant difference existed between the chemical structure of the original BC and the RBC fibers, which meant only physical changes occurred during the whole dissolving and spinning process. The RBC fibers had lower degree of crystallinity and thermal stability than the original BC. The whole fiber showed a round brilliant along the fiber axis with the presence of surface cracks and fibrillation, and possessed relatively poor tensile strength and elongation at break.

Further investigations based on the results can be made on using molten inorganic salts as excellent direct solvents for bacteria cel-

lulose or other polysaccharides, and on more direct applications of BC in different fields, especially in textile industry. More researches should be done to optimize the dissolving process and spinning parameters and to improve the properties of the RBC fibers.

Acknowledgements

This research was financially supported by State Key Laboratory for Modification of Chemical Fibers and Polymer Materials (No. LZ0902).

References

Brown, A. J. (1886). On an acetic ferment which forms cellulose. *Chemical Society*, *49*, 432–439.

Cai, T., Zhang, H., Guo, Q., Shao, H., & Hu, X. (2010). Structure and properties of cellulose fibers from ionic liquids. *Journal of Applied Polymer Science*, *115*, 1047–1053.

Chen, P., Cho, S. Y., & Jin, H. J. (2010). Modification and applications of bacterial celluloses in polymer science. *Macromolecular Research*, *18*, 309–320.

Chen, P., Kim, H.-S., Kwon, S. M., Yun, Y. S., & Jin, H. J. (2009). Regenerated bacterial cellulose/multi-walled carbon nanotubes composite fibers prepared by wet-spinning. *Current Applied Physics*, *9*, e96–e99.

Chen, P., Yuna, Y. S., Baka, H., Cho, S. Y., & Jin, H. J. (2010). Multiwalled carbon nanotubes-embedded electrospun bacterial cellulose nanofibers. *Molecular Crystals and Liquid Crystals*, *519*, 169–178.

Czaja, W. K., Young, D. J., Kawecki, M., & Brown, R. M., Jr. (2007). The future prospects of microbial cellulose in biomedical applications. *Biomacromolecules*, *8*, 1–12.

Fischer, S., Leipner, H., Thümmler, K., Brendler, E., & Peters, J. (2003). Inorganic molten salts as solvents for cellulose. *Cellulose*, *10*, 227–236.

Gao, Q., Shen, X., & Lu, X. (2011). Regenerated bacterial cellulose fibers prepared by the NMMO, H_2O process. *Carbohydrate Polymers*, *83*, 1253–1256.

Gericke, M., Schlufter, K., & Heinze, T. (2009). Rheological properties of cellulose/ionic liquid solutions: From dilute to concentrated states. *Biomacromolecules*, *10*, 1188–1194.

Grinshpan, D. D., Lushchik, L. G. N., Tsygankova, G., Voronkov, V. G., Irklei, V. M., & Chegolya, A. S. (1988). Process of preparing hydrocellulose fibers and films from aqueous solutions of cellulose in zinc chloride. *Fibre Chemistry (English Translation of Khimicheskie Volokna)*, *20*, 365–369.

Heinze, T., Schwikal, K., & Barthellonic, S. (2005). Ionic liquids as reaction medium in cellulose fictionalization. *Macromolecular Bioscience*, *5*, 520–525.

Isogai, A., Usuda, M., Kato, T., Uryu, T., & Atalla, R. H. (1989). Solid-state CP/MAS ^{13}C NMR study of cellulose polymorphs. *Macromolecules*, *22*, 3168–3172.

Laskiewicz, B. (1998). Solubility of bacterial cellulose and its structural properties. *Journal of Applied Polymer Science*, *67*, 1871–1876.

Leipner, H., Fischer, S., Brendler, E., & Voigt, W. (2000). Structural changes of cellulose dissolved in molten salt hydrates. *Macromolecular Chemistry and Physics*, *201*, 2041–2049.

Legnani, C., Vilani, C., Calil, V. L., Barud, H. S., Quirino, W. G., Achete, C. A., et al. (2008). Bacterial cellulose membrane as flexible substrate for organic light emitting devices. *Thin Solid Film*, *517*, 1016–1020.

Liu, R., Shen, Y., Shao, H., Wu, C., & Hu, X. (2001). An analysis of Lyocell fiber formation as a melt-spinning process. *Cellulose*, *8*, 13–21.

Maneerung, T., Tokura, S., & Rujiravanit, R. (2008). Impregnation of silver nanoparticles into bacterial cellulose for antimicrobial wound dressing. *Carbohydrate Polymers*, *72*, 43–51.

Nguyena, V. T., Gidleyb, M. J., & Dykes, G. A. (2008). Potential of a nisin-containing bacterial cellulose film to inhibit listeria monocytogenes on processed meats. *Food Microbiology*, *25*, 471–478.

Nogi, M., & Yano, H. (2008). Transparent nanocomposites based on cellulose produced by bacteria offer potential innovation in the electronics device industry. *Advanced Materials*, *20*, 849–1852.

Phisalaphong, M., Suwanmajo, T., & Sangtherapitikul, P. (2008). Novel nanoporous membranes from regenerated bacterial cellulose. *Journal of Applied Polymer Science*, *107*, 292–299.

Shen, X., Ji, Y., Wang, D., & Yang, Q. (2010). Solubility of a high molecular-weight bacterial cellulose in lithium chloride/N, N-dimethylacetamide solution. *Journal of Macromolecular Science Part B: Physics*, *49*, 1012–1018.

Zhang, J., Luo, J., Tong, D., Zhu, L., Dong, L., & Hu, C. (2009). The dependence of pyrolysis behavior on the crystal state of cellulose. *Carbohydrate Polymers*, *79*, 164–169.

Zaborowska, M., Bodin, A., Bäckdahl, H., Popp, J., Goldstein, A., & Gatenholm, P. (2010). Microporous bacterial cellulose as a potential scaffold for bone regeneration. *Acta Biomaterialia*, *6*, 2540–2547.